Effect of Iron Availability on the Growth and Microcystin Content of Natural Populations of *Microcystis* spp. from Reservoirs in Central Argentina: A Microcosm Experiment Approach

Silvana Raquel Halac [1,2,*] , Ana Laura Ruibal-Conti [1,3,*] , Luciana del Valle Mengo [2] , Florencia Ullmer [1], Aldana Cativa [1], Raquel Bazan [4] and Maria Ines Rodriguez [1]

[1] Instituto Nacional del Agua, Centro de la Región Semiárida (INA-SCIRSA), Ambrosio Olmos 1142, Córdoba X5000JGT, Argentina

[2] Centro de Investigaciones en Ciencias de la Tierra, Consejo Nacional de Investigaciones Científicas y Técnicas (CONICET), Av. Vélez Sarsfield 1699, Córdoba X5016GCN, Argentina

[3] Facultad de Química, Universidad Católica de Córdoba, Av. Armada Argentina 3555, Córdoba X5016DHK, Argentina

[4] Facultad de Ciencias Exactas, Físicas y Naturales, Universidad Nacional de Córdoba (UNC-FCEFyN), Av. Vélez Sarsfield 1611, Córdoba X5016GCN, Argentina

* Correspondence: silvana.halac@unc.edu.ar (S.R.H.); aruibal@ina.gob.ar (A.L.R.-C.); Tel.: +54-351-5353800 (S.R.H.); Fax: +54-351-4344980 (S.R.H.)

Abstract: The eutrophication of aquatic systems is a problem related to the contribution of excess nutrients—phosphorus (P) and nitrogen (N)—to water bodies, which produces an increase in cyanobacterial blooms. Under eutrophic conditions, P and N concentrations are sufficient for cyanobacteria growth, and some micronutrients are considered to become limiting for population growth. This work aimed to assess the effect of iron on cyanobacteria growth and the content of MCs in natural populations of *Microcystis* spp. Microcosm setting experiments were carried out with natural samples collected during two bloom events of *Microcystis* spp., kept under controlled light, temperature and pH conditions. The first bloom sample was exposed to different iron concentrations (400, 700 and 1100 µg Fe·L^{-1}) to determine the optimum concentration for growth. The second was exposed to different iron addition modes (one: T1P, and two pulses: T2P) to imitate the iron increase produced by the downward migration of *Microcystis* spp. colonies. Our results show that iron is a growth-promoting factor and that its optimal range of concentrations for the growth of *Microcystis* spp. under the experimental setting conditions is between 700 and 1100 µg Fe·L^{-1}. On the other hand, growth rates were not significantly different between T1P and T2P; thus, different addition modes did not have an effect on growth. Regarding microcystin content, the MC quota in natural populations of *Microcystis* spp. did not show a clear relationship with the iron supply. This work contributes to the understanding of the underlying factors affecting cyanobacteria bloom formation and the production of MCs, which in turn would impact the development of management strategies to control cyanobacteria blooms.

Keywords: eutrophic waters; cyanobacteria bloom; iron; anoxic hypolimnion; microcystin quota

1. Introduction

Anthropogenic eutrophication is a serious water quality problem affecting fresh and brackish waterbodies worldwide [1–3]. It is associated with high inputs of phosphorus (P) and nitrogen (N) compounds from human activities in the watershed [4–6]. One of the consequences of eutrophication is the massive development of cyanobacteria (phenomena known as cyanobacteria blooms), which alters the normal equilibrium of the aquatic ecosystem [7]. Additionally, some groups of cyanobacteria can produce toxic metabolites that

affect animal and human health and represent a serious risk for public health. Cyanobacteria blooms generally occur seasonally, but climate change conditions are expected to exacerbate them, leading to more intense and permanent blooms and to serious impairment of the water quality used as a drinking supply or for recreational purposes [3,8–10].

Microcystis spp. is a unicellular cyanobacteria normally clustered in colonies of different morphologies and capable of producing toxic metabolites known as microcystins (MCs) [11]. *Microcystis* blooms and MCs are globally distributed, and their presence has been reported in many countries worldwide [12,13]. Argentina is not exempt from this problem, and drinking water reservoirs of important urban areas located in semiarid regions are particularly vulnerable to the impact of toxic *Microcystis* blooms [14–16].

Despite numerous studies carried out to date, the ecological role of MCs and the causes of their production are still unclear. It is well known that the growth and MC content of *Microcystis* spp. populations are greatly influenced by a number of environmental factors. Numerous studies have examined the effect of light and temperature [17–19], pH [20] and macronutrients (P and N) [21–24] on growth and MC production. Metal ions are other significant chemical factors, of which their comprehensive impact is still being studied [25–28].

Under optimal light and temperature conditions, it has been observed that *Microcystis* spp. blooms can be regulated by the concentration of P and N, as well as the N/P ratio [22,29,30]. However, in natural conditions, under eutrophic or hypereutrophic circumstances, the concentrations of P and N, as well as the ratio N/P, are within the required concentrations for cyanobacterial growth, so other elements become important. In the case of cyanobacteria, iron is one of the micronutrients with the highest requirements, and generally, this group has a higher demand for iron than eukaryotic cells [31,32]. This metal is incorporated into cyanobacteria cells in the form of ferrous iron (Fe^{2+}), which is the oxidative status in which iron can be transported through its membrane. Molot et al. [33] proposed that the availability of Fe^{2+} is important for the ability of cyanobacteria to outcompete eukaryotic algae and for bloom formation. They suggest that some colonial cyanobacteria (e.g., *Microcystis* spp.) can move to bottom waters through changes in buoyancy and obtain the iron (Fe^{2+}) normally released from the sediments of anoxic nutrient-rich waters. This mechanism would prevent the deficit of iron inside the cyanobacteria cells, which is an advantage for their growth over the other phytoplankton groups.

Regarding the production of MCs, Dai et al. [26] reviews the environmental factors that influence the synthesis of MCs. Iron has also been postulated to influence the production of MCs in different ways.

One hypothesis supports the idea that MCs would act as an intracellular iron chelator [19] or as an extracellular iron-scavenging molecule [34], and as such, the iron concentration in water would directly regulate the synthesis of MCs [35]. When the iron concentration in water is low, cells would synthesize more MCs [28,36–38], which in turn would act as an iron chelator, either scavenging the available iron and facilitating its uptake or storing it inside the cell.

Extensive research has been performed to study *Microcystis* spp. bloom formation and the ecophysiological role of MCs, as well as the effect of environmental parameters on the regulation of population growth and the production of MCs. Most of this research has consisted of either culture-based studies using pure cyanobacteria strains under controlled conditions or field studies using natural cyanobacteria populations under natural conditions (see [39] and references therein). Only a few studies have been carried out with natural populations under laboratory controlled conditions. The relevance of these types of studies is that they maintain the colony aggregation of *Microcystis* spp. and they control some environmental factors in optimal ranges for growth. On the contrary, if these colonies are transferred to the laboratory and isolated, they disaggregate into a unicellular form after some generations [40]. In addition, some authors suggested that colonial *Microcystis* has a higher tolerance to stress conditions when compared to unicellular phenotypes [41,42].

Hence, by using natural populations, we expect that our experiments may reflect the response of *Microcystis* spp. in lakes better than those experiments using axenic cultures.

In this work, we used natural populations of *Microcystis* spp. collected from two eutrophic reservoirs in a semiarid region of central Argentina in order to evaluate the response of local populations to changes in the iron concentration under controlled laboratory conditions. We evaluated the effect of the iron concentration on population growth and MC content. It is known that colonies of *Microcystis* spp. are able to move downward in the water column for better acquisition of nutrients in the anoxic hypolimnion (e.g., soluble iron—Fe^{2+}; [33]). For this reason, we considered not only the iron concentration in water but also different modes of supplying it as experimental treatments, simulating one or two sudden iron pulses. The iron pulse might reproduce the iron increase produced when *Microcystis* spp. colonies move to bottom layers during anoxic conditions.

Despite the importance of *Microcystis* spp. blooms in reservoirs in central Argentina, few experimental studies have been conducted for identifying the main drivers controlling these bloom events. The aim of this work was to assess the effect of iron on cyanobacteria growth and MC content in natural populations of *Microcystis* spp. The study focused on answering some questions raised in eutrophic systems: (1) which is the optimum range of iron concentrations for the growth of natural populations of *Microcystis* spp.? (2) Is there a positive effect on growth if iron is supplied in two pulses instead of only one (simulating one or two downward migration events along the population growth)? (3) Might MC content be affected by different iron concentrations and supply modes?

This study attempts to contribute to the understanding of the underlying factors affecting cyanobacteria growth and MC production and their relationship with internal nutrient dynamics in eutrophic reservoirs. In turn, this would contribute to freshwater management and the effective application of strategies to control cyanobacteria blooms.

2. Materials and Methods

2.1. Microcystis spp. Collection, Sample Characterization and Laboratory Acclimation

Microcystis spp. populations were obtained from the center area of two eutrophic reservoirs in the semiarid region of central Argentina (Pampean Ranges of Córdoba; [43]) during bloom events in March 2017 and February 2018. Simultaneously to the sampling, air and water temperature, conductivity, pH and dissolved oxygen were measured in situ with a multiparametric probe (YSI model 556 MPS). Samples for microcosm experiments and for determination of the phytoplankton composition, total phosphorus, inorganic nitrogen and chlorophyll *a* were collected at a depth of 0.10 m in 5 L acid-washed (HCl 1N) opaque plastic bottles and transported to the laboratory at 4 °C in dark conditions within 3 h.

The characterization of the phytoplankton community was made at the laboratory immediately by counting an aliquot of the sample with a compound microscope (see more details in Section 2.3). Determination of most of the nutrients was performed at the laboratory following the Standard Analytical Methods (APHA 2017): total phosphorus (TP; SM 4500-P E); nitrites (SM 4500-NO_2 B), nitrates (SM 4110 B) and ammonium (SM 4500-NH_3 A–G). Dissolved inorganic nitrogen (DIN) was estimated as the sum of the three N-fractions.

Microcystis spp. colonies were kept at the laboratory in fish tanks under natural light (~42 $\pm$ 10 μE·m^{-2} s^{-2}) and at room temperature for 15–30 days (~22 $\pm$ 2 °C) before commencing the experiments for indoor acclimation. The phytoplankton composition did not change during this period and *Microcystis* spp. continued to be dominant, as confirmed through cellular counts carried out the day before starting the experiments. Cell counting was also performed for calculating a mean volume of the inoculum for reaching a concentration of *Microcystis* spp. corresponding to natural blooms reported in the region [15,44].

2.2. Experimental Design

Given the difficulty of working in the field with natural populations of *Microcystis* spp., the experimental design tried to reproduce, in the laboratory, the natural physicochemical characteristics of the subsurface layer of the water column during the austral seasons of summer and autumn. The physicochemical characteristics of the experiments were defined by taking into account mean values of the water quality data obtained from the periodic monitoring of the reservoir most studied in the region, the San Roque reservoir (SRr), during the 1999–2018 period (Table 1). The conditions of temperature, TP and soluble iron (SFe) concentration in SRr during blooms of *Microcystis* spp. were specially considered. The SRr was also selected as a "model system" because of its eutrophic state, the frequent blooms of cyanobacteria (mainly *Microcystis* spp. and *Dolichospermum* spp.) occurring during late spring, summer and autumn seasons and the consequent hypolimnetic anoxia and fish death events [44]. Information on the land use and physical characteristics of the SRr and its watershed can be found in [45].

Table 1. Physicochemical characteristics of the San Roque reservoir in spring (S_p), summer (S_u) and autumn (A) at the center of the reservoir (for the subsurface and deepest layers of the water column). Monthly measurements obtained from the period 1999–2018 are presented as median, minimum and maximum values. Data were provided by the Continuous Program of Water Quality Monitoring (INA-SCIRSA).

Physiochemical Variables in S_p, S_m and A		Subsurface Layer (0.5 m below Surface)			Deepest Layer (1 m above the Bottom)		
		Median	Min	Max	Median	Min	Max
Water temperature (°C)	S_p	21.3	13.1	27.6	18.7	12.9	21.1
	S_u	24.6	21.1	28.7	22.8	16.7	25.9
	A	18.9	12.0	24.5	18.4	11.5	23.4
Conductivity (μS·cm^{-1})	S_p	272	194	492	267	103	494
	S_u	213	128	335	180	76.6	329
	A	178	100	338	178	108	336
pH	S_p	8.2	6.5	9.8	7.6	6.1	9.2
	S_u	8.4	6.8	9.7	7.2	6.1	8.5
	A	7.6	6.0	9.2	7.6	6.1	8.5
Dissolved oxygen (mg·L^{-1})	S_p	9.3	2.8	15,3	4.7	0.0	11.3
	S_u	8.4	4.4	16.7	1.0	0.0	9.6
	A	8.0	3.7	22.3	6.7	0.0	11.1
Total phosphorous (μg·L^{-1})	S_p	66	14	392	61	10	322
	S_u	94	10	1117	127	30	420
	A	74	35	240	76	27	756
Dissolved inorganic nitrogen (μg·L^{-1})	S_p	435	143	849	532	146	1248
	S_u	147	56	570	345	85	975
	A	346	138	655	376	146	713
Total iron (μg·L^{-1})	S_p	120	$\leq$50	830	160	$\leq$50	1300
	S_u	120	$\leq$50	950	290	$\leq$50	2600
	A	140	$\leq$50	310	180	$\leq$50	1570
Chlorophyll *a* (μg·L^{-1})	S_p	25.0	$\leq$2.0	876	3.3	$\leq$2.0	114
	S_u	78.2	$\leq$2.0	1068	4.1	$\leq$2.0	88
	A	27.1	$\leq$2.0	482	6.0	$\leq$2.0	186

We used an "enclosed ecosystem" (hereinafter microcosm) as a biological model that simplifies and simulates complex and heterogeneous natural ecosystems ([46] and references therein). Inside microcosms we isolated and incubated a water parcel collected from the lake under conditions similar to those found in the natural environment. This setting made it possible to conduct controlled incubations of natural populations of *Microcystis* spp., regulating nutrients, temperature and light, in optimal ranges for growth. Natural conditions are not completely simulated in these cases; for example, water movements are restricted. In these types of microcosm experiments, phytoplankton biomass tends to increase rapidly and therefore often reproduces bloom conditions [47].

After *Microcystis* spp. bloom events occurred during March 2017 and February 2018, two microcosm experiments were carried out during April 2017 (first experiment, sample-2017) and April 2018 (second experiment, sample-2018). For both experiments, an aliquot (20–50 mL) of *Microcystis* spp. natural populations maintained under room conditions (as described in Section 2.1) were incubated in 2 L transparent polyethylene bags (microcosms) that contained filtrated and autoclaved sterilized water from the SRr. The microcosms were placed in a plastic tank (50 L) with tap water under controlled temperature at 27 ± 0.35 °C maintained by a water heater (Aqua Zonic AZ Easy Heater) and also under a photosynthetically active radiation intensity of 43.5 ± 3.2 $\mu E \cdot m^{-2}$ s^{-2} provided by a fluorescent array with a light/dark regimen of 12 h:12 h. Lamps were located above the incubation tank for avoiding the shade effect and for obtaining an homogeneous light field. The experiment design consisted of a unique tank containing three microcosms (replicates) of each of the experiment treatments and control. Microcosms were shaken every day to obtain a homogeneous sample, and they were rearranged randomly to reduce the minor differences in photon irradiance. Initial cell densities for both experiments were selected to be inside the range of *Microcystis* spp. natural blooms historically reported in SRr ([44]) and observed during the bloom events of 2017 (3.0×10^7–1.5×10^8; [48]).

The first experiment was carried out during April 2017 for testing the optimal iron concentration for *Microcystis* spp. growth. Four iron treatments were established: (a) Control, without iron addition: natural iron concentration in the water used in experiments = 27 ± 5 μg $Fe \cdot L^{-1}$ (0.5 μM); (b) TI: +400 μg $Fe \cdot L^{-1}$ (7 μM); (c) TII: +700 μg $Fe \cdot L^{-1}$ (12 μM); (d) TIII: +1100 μg $Fe \cdot L^{-1}$ (20 μM). The three iron concentrations are representative of natural conditions and were selected considering concentrations above the median (120 μg $Fe \cdot L^{-1}$) and maximum values (950 μg $Fe \cdot L^{-1}$) in the SRr subsurface layer during the summer season (Table 1). The initial inoculum of *Microcystis* spp. added to each microcosm made it possible to reach an initial cell abundance of $1.3 \pm 0.4 \times 10^8$ cells·L^{-1}. The experimental period lasted for 26 days and included the initial lag stage and the exponential stage of algal growth. The end of the exponential stage was confirmed based on the optical density (OD, absorbance at 750 nm, Shimadzu spectrophotometer model UV-1700, Japan) measured daily over the whole experiment ([49]).

The second experiment was carried out during April 2018 for testing the response of cyanobacterial growth to different iron addition modes (one or two pulses). The iron concentration was selected based on the most favorable concentration of iron for cyanobacterial growth in the first experiment. The two-pulse design aims to reproduce the increase in iron due to the downward migration of cyanobacteria colonies to deeper anoxic layers in eutrophic systems (e.g., median and maximum total iron values at SRr's hypolimnion during summer season: 290 and 2600 $\mu g \cdot L^{-1}$, respectively; Table 1). The treatment setting was as follows: (1) Control, without iron addition: natural iron concentration measured in water used in experiments = 179 ± 25 μg $Fe \cdot L^{-1}$ (3 μM); (2) Treatment 1 Pulse (T_{1P}): +700 μg $Fe \cdot L^{-1}$ (12 μM) at day 1 (D1); Treatment 2 Pulses (T_{2P}): the same amount divided in 2, +350 μg $Fe \cdot L^{-1}$ (6 μM) at D1 (first pulse) and 350 μg $Fe \cdot L^{-1}$ at day 9 (D9; second pulse). The second pulse was set on day 9 since we considered it close to the start of the exponential growth. On the first experimental day, each microcosm was inoculated with an aliquot of *Microcystis* spp., and the initial cell abundance was $2.5 \pm 0.7 \times 10^7$ cells·L^{-1}.

The experimental period lasted for 25 days. As in the previous experiment, the second experiment included lag and exponential stages of algal growth.

For both experiments, the iron solution was prepared by mixing 10 mL of $FeCl_3$ (0.2 M) in HCl (pH: 2) with 20 mL of disodium EDTA solution in NaOH (pH: 7; 0.2 M). The final pH of the solution of $FeCl_3$ in EDTA was 6. Under these conditions, EDTA and the iron cation Fe^{3+} form a strong coordination complex and iron does not precipitate ([50]). To avoid phosphorus limitation due to the consumption by cells over the experiment, K_2HP0_4 was added to each microcosm to reach a final concentration of 100 µg P. L^{-1}, according to the median total TP value in the SRr subsurface layer during the summer season (Table 1).

2.3. Physicochemical and Biological Determinations of Microcosm Samples

During the experiments, physicochemical parameters (water temperature, conductivity, pH and dissolved oxygen) were measured in situ using a multiparametric probe (YSI model 556 MPS) in each microcosm. After mixing the whole content of each microcosm, 70 mL of water was collected with a syringe to determine soluble reactive phosphorus (SRP), SFe, cell abundance and microcystin (MC) content. Sampling was carried out early in the morning during experimental days 1, 5/4, 8, 14/15 and 25/26 during the first (sample-2017) and second experiment (sample-2018), respectively.

Samples for determining SRP and SFe were previously filtered using a Millipore cellulose acetate membrane filter (pore size 0.45 mm; Ø = 47 mm) and preserved at −20 °C and 4 °C, respectively. Samples for determining SFe were preserved with HNO_3 (0.1%; *v/v*). SRP was determined following the Standard Analytical Methods ([51]; 4500-P E), and absorbances were measured in a spectrophotometer (Shimadzu UV-1700) at 880 nm. The SFe concentration was measured by adjusting the volume of each sample to 25 mL with Milli-Q water and analyzing it via atomic absorption spectrometry (AAS), using a Perkin Elmer Spectrophotometer Model AA 3110.

Microcystis spp. samples for cell abundance determination were fixed in buffered formalin (0.4% final concentration, *v:v*), and maintained in the dark at 4 °C. For quantification, samples were mixed well, and an aliquot of 1 mL was taken and dispensed into a Sedgewick–Rafter chamber. Duplicate samples from each experimental replicate were observed with a compound microscope (Zeiss model D-7082, Germany) using 200× magnification. Counts were made along transects until at least 20 colonies were observed. The height, width and thickness of each colony were measured and assimilated to known geometric forms in order to estimate the volume ([52]). The individual volumes of 10 cells were also measured for each sample. The cell abundance was estimated as follows:

$$CA_{\text{sample } x} = [(\sum CoV_{\text{sample } x})/(\overline{X}\, CeV_{\text{sample } x})]/VoT \qquad (1)$$

where $CA_{\text{sample } x}$ is the cell abundance of sample x, $CoV_{\text{sample } x}$ and $CeV_{\text{sample } x}$ are the colony and the cell volumes, respectively, and VoT corresponds to the total volume of transects.

The growth of populations of *Microcystis* spp. throughout the experiments was simultaneously followed using the absorbance of samples in vivo, for identifying the start and the end of the exponential growth phase. Absorbance was measured each sampling day using a spectrophotometer (Shimadzu UV-1700) at 750 nm ([49]).

Samples for total MC analyses were taken as 2 mL sub-samples of the bottle collected for phytoplankton analysis. Sub-samples were collected after complete homogenization of the sample and stored in plastic vials at −20 °C. Total MCs were determined via an immuno-enzymatic assay (ELISA Kit, Abraxis, detection limit = 0.15 µg·L^{-1}), which detects all variants of MCs due to its capacity to bind specifically to the ADDA moiety present in all MC congeners. Sub-samples were subjected to a pretreatment of three thaw–freeze cycles (to lyse the cells and release the MCs) and then filtered through acetate–cellulose membrane filters (pore size, 0.45 µm; Ø = 13 mm) to remove detritus (remaining broken cells) and to recover the soluble MCs. As MCs are intracellular peptides and are not actively

excreted by cyanobacteria cells, using this procedure, it is possible to calculate the average amount of MCs per cell (MC quota). The MC quota was then calculated as the total MC concentration over *Microcystis* spp. cell abundance.

$$\text{MC quota}_{\text{sample } x} = [\text{MCs}]_{\text{sample } x} / \text{CA}_{\text{sample } x.} \tag{2}$$

where MC quota$_{\text{sample } x}$ is the average amount of MCs per cell or the quota of sample x, $[\text{MCs}]_{\text{sample } x}$ is the MC concentration, and $\text{CA}_{\text{sample } x}$ is the cell abundance, as in Equation (1).

2.4. Data and Statistical Analysis

Iron treatments were performed in triplicate. All data are reported as the mean and standard deviation.

The specific growth rate (μ) of *Microcystis* spp. populations was calculated from the cell abundance during the exponential phase according to the following:

$$\mu \ (d^{-1}) = \text{Ln} \ (N_f/N_i)/(t_f - t_i) \tag{3}$$

where N_f and N_i are the cell abundance on the last and first day, respectively, during the exponential growth phase and $(t_f - t_i)$ is the duration of this phase in days.

The rates of SFe and SRP decrease were determined from the slope of a linear regression throughout the whole experiment.

A one-way ANOVA test was performed to determine differences in the cell abundance, growth rate, SRP and SFe decrease, MC concentration and MC quota among iron treatments for each day, using a significance level (α) of 0.05 for all comparisons ([53]). Subsequently, a Tukey test was performed to distinguish the treatments with significantly different effects. The normality and homoscedasticity of data were checked using the Shapiro–Wilk test and Breusch–Pagan test, respectively. In all cases, R v. 3.6.3 software ([54]) was employed.

3. Results and Discussion

3.1. Characterization of Phytoplankton Community during Microcystis spp. Blooms

The sample obtained from the bloom during March 2017 was mostly composed of *Microcystis* spp. (95.2%); other species of Dinophyceae, Diatomeae, Chlorophyceae and Cryptista were also present and represented a low percentage of the total phytoplankton community (Table 2). This population presented a very low concentration of MCs (range: 0.1 to 0.6 $\mu g \cdot L^{-1}$) and also low MC quota values ($0.27 \pm 0.05 \times 10^{-2}$ pg·cell^{-1}).

The sample obtained during February 2018 mostly constituted *Microcystis* spp. (97.3%); other species of Cyanobacteria, Diatomeae, Chlorophyceae, Zygnematophyceae and Cryptista were also detected but contributed to a low proportion of the total phytoplankton community (Table 2). Regarding the potential toxicity, the sample-2018 presented both high concentrations of MCs ($5.7 \pm 0.9 \ \mu g \cdot L^{-1}$) and high MC quota values (0.18 ± 0.02 pg·cell^{-1}), which were within the range of other studies with natural *Microcystis* spp. populations ([39,55]). In both samples, the inspection using an optic microscope made it possible to confirm that the cells were in good condition.

3.2. Physicochemical Conditions during Microcosm Experiments

Environmental conditions inside the microcosms throughout the experiment were maintained in ranges between minimum and maximum values measured at the subsurface layer of the SRr during the summer season (1999–2018; Table 1). During both experiments, pH varied from 7 to 8, conductivity ranged from 0.15 to 0.28 Ms·cm^{-1} and dissolved oxygen displayed values between 6 and 8 mg·L^{-1}. These conditions were similar for all the treatments and are representative of SRr´s subsurface layer during the summer season (Figure 1 and Table 1).

Table 2. Characterization of phytoplankton community during *Microcystis* spp. bloom collected for microcosm experiments in March 2017 (sample-2017) and February 2018 (sample-2018).

Phytoplankton Composition at the Reservoir Center		Cell Abundance (Cell·L^{-1})	Contribution to Total Abundance (%)
sample-2017			
Cyanobacteria	*Microcystis* spp.	3.0×10^7	95.2
Dynophyceae	*Ceratium furcoides*	1.2×10^6	3.81
Diatomeae	*Aulacoseira granulata*	1.0×10^5	0.32
	Cyclotella sp.	1.8×10^5	0.57
Chlorophyceae	*Monorraphydium* sp.	3.3×10^4	0.10
Cryptista	*Cryptomonas* sp.	2.0×10^3	0.006
sample-2018			
Cyanobacteria	*Microcystis* spp.	7.3×10^7	97.3
	Aphanocapsa sp.	1.8×10^6	2.40
	Dolichospermum spp.	3.7×10^5	0.49
Diatomeae	*Cyclotella* sp.	8.5×10^3	0.01
	Nitzschia sp.	1.4×10^3	0.002
Chlorophyceae	*Pediastrum* sp.	3.4×10^4	0.04
Zygnematophyceae	*Staurastrum* sp.	4.2×10^3	0.005
Cryptista	*Chroomonas* sp.	2.5×10^4	0.05
	Cryptomonas sp.	1.4×10^3	0.002

Experimental conditions were in accordance with those optimal for the growth of *Microcystis* spp. previously reported by several authors at different locations: temperatures within a range of 25–32 °C, alkaline pH values and light intensities of 40 to 280 µE·m^{-2}·s^{-1} [17,18,56–58]. Elevated temperatures are frequently associated with *Microcystis* spp. blooms with stratification conditions of the water column, which is more favorable for the growth of populations than the mixing condition, as observed in the SRr [57]. Water column stratification frequently occurs at the SRr during the summer [44].

3.3. Effect of Iron Availability on Microcystis spp. Growth

3.3.1. Microcosm Experiment Testing Different Iron Concentrations

Natural populations of *Microcystis* spp. collected in March 2017 exhibited differences in growth when supplied with different iron concentrations (TI: 400 µg Fe·L^{-1} = 7 µM, TII: 700 µg Fe·L^{-1} = 12 µM and TII: 1100 µg Fe·L^{-1} = 20 µM) or when compared to that with no addition (control treatment: 27 µg Fe·L^{-1} = 0.5 µM). In particular, *Microcystis* spp. populations supplied with iron reached higher cell abundance by the end of the experiment than those without an iron supply (Figure 2A). Moreover, cells supplied with 700 and 1100 µg Fe·L^{-1} exhibited significantly higher specific growth rates throughout the exponential phase than cells under control and TI (400 µg Fe·L^{-1}) conditions ($p \leq 0.05$; Table 3). Similar results were reported by other studies that observed higher *M. aeruginosa* growth rates under iron-replete (28–100 µM) conditions in comparison with those under iron-depleted conditions (0.1 µM) [59,60].

In accordance with *Microcystis* spp. growth, the SFe and SRP concentration decreased throughout the experiment with the three iron addition treatments (Figure 2B), but the rates of decrease were not significantly different among them (Table 3; $p > 0.05$). The decrease in SRP and SFe concomitant with an increase in *Microcystis* spp. growth would indicate the consumption of these elements by the cells. As Fe^{3+} forms a very strong 1:1 molar coordinating complex with EDTA, in neutral-alkaline conditions, the precipitation of Fe^{3+} in water is discarded.
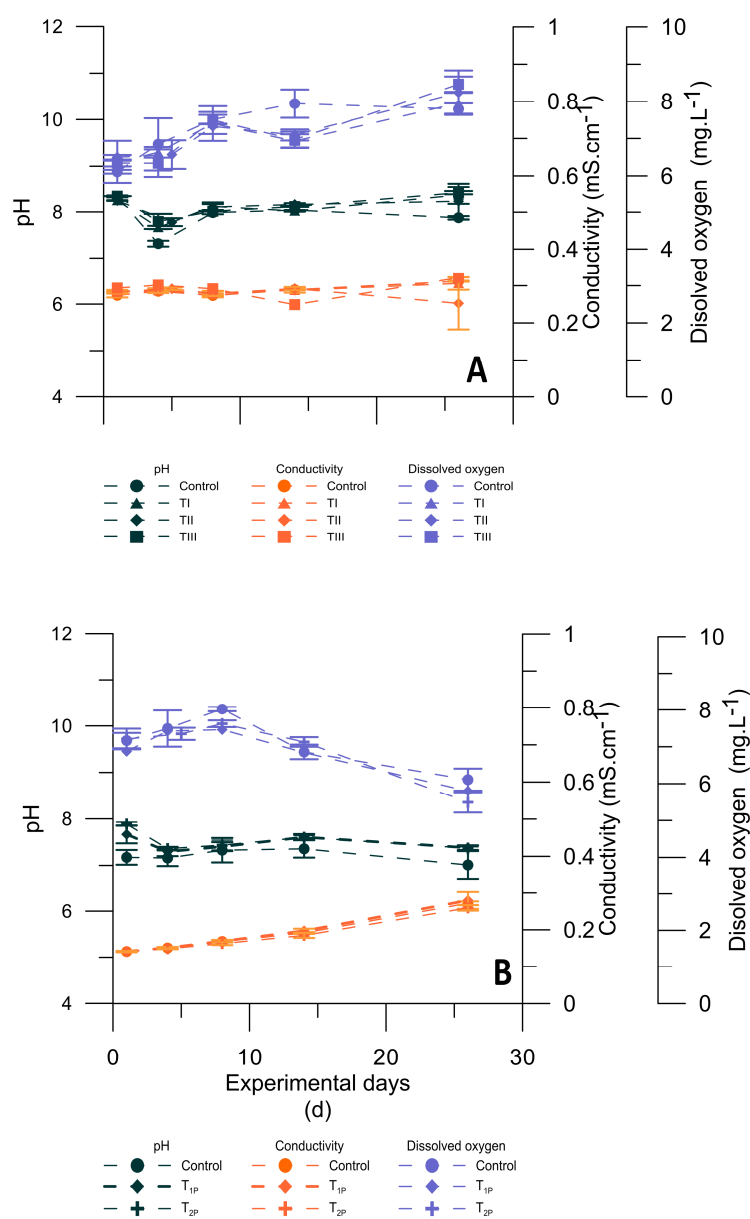
Figure 1. Physicochemical variables recorded in situ at each microcosm during the first experiment (sample-2017; (**A**)) and the second experiment (sample-2018; (**B**)): dissolved oxygen (mg·L^{-1}), pH and conductivity (mS·cm^{-1}). Values are the means of triplicates, and vertical lines on the top of symbols represent the standard deviations.

According to our results and to iron values registered at subsurface layers of the SRr during the seasons with most frequent blooms (e.g., summer: ~50 to 950 and autumn: ~50 to 310 µg Fe·L^{-1}; Table 1), iron may not be at an optimal concentration for the growth of *Microcystis* spp. most of the time. Instead, the greater availability of iron at deeper layers (~50 to 2600 and 50 to 1570 µg·L^{-1} for summer and autumn, respectively; Table 1) might be an important resource for the growth of cyanobacteria populations. This may be caused by the release of Fe^{2+} from the sediment to the water column, a process that is favored by the anoxic conditions present at the deepest layer during spring, summer and autumn (see dissolved oxygen values at hypolimnion in Table 1). The variability in the iron concentration in the water column can be exploited by species with the ability to move to different depths (e.g., *M. aeruginosa*; [61,62]). Hence, *Microcystis* colonies may take advantage of sudden increases in the availability of iron by moving to anoxic bottom waters [33].
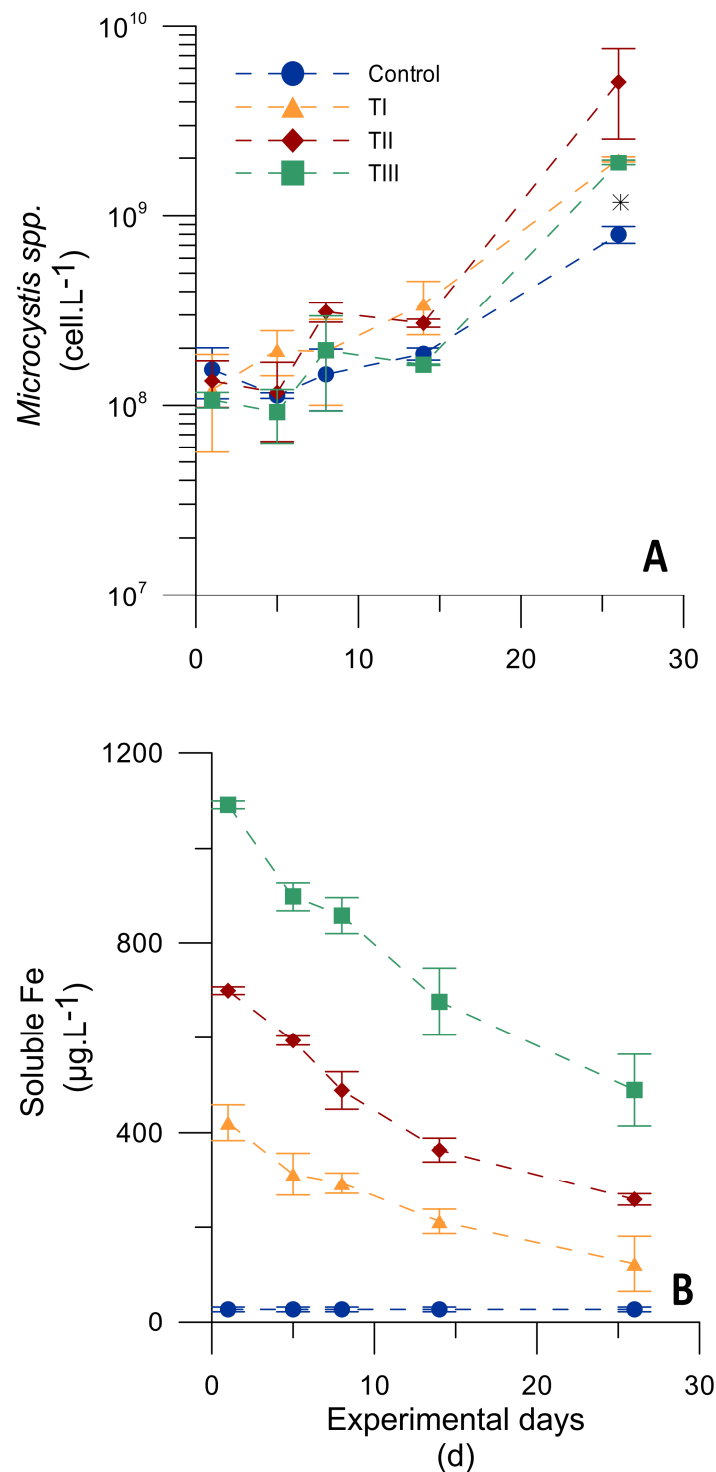
Figure 2. Cell abundance (cell·L^{-1}) (**A**) and soluble iron concentration (µg·L^{-1}) (**B**) in *Microcystis* spp. natural populations from sample-2017 under different treatments during the first experiment. Control, without iron addition (27 ± 5 µg Fe·L^{-1}); TI: +400 µg Fe·L^{-1}; TII: +700 µg Fe·L^{-1}; TIII: +1100 µg Fe·L^{-1}. Values are the mean of triplicates, and vertical lines above symbols are standard deviations. Asterisks are located above the treatments that showed a significant difference in cell abundance in comparison with that in the other treatment groups (**A**).

Table 3. *Microcystis* spp. natural samples collected from the 2017 bloom: specific growth and soluble iron decreasing rates in microcosms exposed to different iron treatments: control, without iron addition; TI, 400 µg·L-1; TII, 700 µg·L-1; TIII, 1100 µg·L-1. The mean and standard deviation of growth and decreasing rate values resulted from triplicate microcosms. Different letters indicate significant differences among treatments. SFe: soluble iron; SRP: soluble reactive phosphorus; *n.d.*: not detectable.

Iron Treatments	Specific Growth Rate (μ) during the Last 12 Days (d^{-1})	SFe Decreasing Rate throughout the Experiment [(µg·L^{-1})·d^{-1}]	SRP Decreasing Rate throughout the Experiment [(µg·L^{-1})·d^{-1}]
Control (no iron addition)	0.121 ± 0.002 (a)	*n.d.*	−3.02 ± 0.94 (a) r^2 = 0.68
TI (400 µ Fe·L^{-1})	0.147 ± 0.017 (a)	−17.95 ± 0.64 (a) r^2 = 0.87	−3.19 ± 0.71 (a) r^2 = 0.68
TII (700 µ Fe·L^{-1})	0.239 ± 0.028 (b)	−21.77 ± 0.46 (a) r^2 = 0.95	−4.12 ± 0.61 (a) r^2 = 0.88
TIII (1100 µ Fe·L^{-1})	0.204 ± 0.002 (b)	−28.37 ± 6.89 (a) r^2 = 0.98	−4.96 ± 0.22 (a) r^2 = 0.95

In this line, a subsequent experiment testing the response to differential iron addition modes (one or two pulses) was conducted. For this purpose, based on the results of the first experiment showing that cells supplied with 700 and 1100 µg Fe·L^{-1} exhibited similar growth rates, 700 µg Fe·L^{-1} was chosen as the total iron concentration for testing different pulses.

3.3.2. Microcosm Experiment Testing Different Iron Pulses

Samples of *Microcystis* spp. collected during February 2018 were supplied with 700 µg Fe·L^{-1} in different ways. Treatment 1 (T_{1P}) consisted of one pulse of 700 µg Fe·L^{-1}, while treatment 2 (T_{2P}) consisted of two pulses of 350 µg Fe·L^{-1} each. During the exponential phase, populations of *Microcystis* spp. displayed a significantly higher specific growth rate in the iron addition treatment groups in comparison with that in the control ($p \leq 0.05$; Table 4). However, there were no significant differences in the specific growth rate between the iron addition treatments (T_{1P} and T_{2P}; Figure 3 and Table 4). Along with population growth, SFe and SRP displayed a decrease of their concentrations, as observed based on their negative decreasing rates (Table 4). The decreasing SRP rates measured throughout the experiment did not show significant differences between control and iron treatments. These results, along with those observed in the first experiment, confirmed that P was not completely consumed in either of the two experiments, so it is considered a non-limiting factor for the growth of the *Microcystis* spp. populations. As was also observed in the first experiment, SFe decreasing rates were not significantly different between iron treatments, in this case, considering the rates estimated before the second pulse (D1 to D8; Table 4).

Extensive research has demonstrated that, in general, nutrient-rich waters have anoxic sediments, conditions favored by warm temperatures and stable water columns [63,64]. Hypolimnetic anoxia was reported to promote cyanobacteria blooms in eutrophic waters by promoting Fe^{2+} release from sediments and the concurrent availability for cyanobacteria. As Fe^{2+} transported upward from anoxic sediments remains in a reduced form until it reaches oxygenated waters—where it is rapidly oxidized to Fe^{3+}—cyanobacteria must migrate downwards into anoxic waters below the mixed layer to acquire internally loaded Fe^{2+} before its reoxidation [33]. Indeed, the downward migration of cyanobacteria into anoxic waters has been observed ([65] and references therein), and *M. aeruginosa* colony velocities have been measured as 52 ± 13 m·day^{-1} [61]. However, other hypotheses have been formulated for algal buoyancy in natural systems and appear to be much more

dependent on light than on nutrients. In this case, physical mechanisms may provide the sufficient replenishment of nutrients at epilimnion from hypolimnion layers, explaining the maintenance of high growth rates of epilimnetic phytoplankton populations [66].

Table 4. *Microcystis* spp. natural samples collected from the 2018 bloom: specific growth and soluble iron decreasing rates in microcosms exposed to different iron treatments: control, without iron addition; with different iron addition treatments: T_{1P}, one pulse of 700 µg·L^{-1}; T_{2P}, two pulses of 350 µg·L^{-1} each. The mean and standard deviation of growth and decreasing rate values resulted from triplicate microcosms. Different letters indicate significant differences among treatments. SFe: soluble iron; SRP: soluble reactive phosphorus; *n.d.*: not detectable. Period considered: * D1–D25; ** D1–D8 (before the second iron pulse).

Iron Treatments	Specific Growth Rate (μ) during the Last 11 Days (d^{-1})	SFe Decreasing Rate throughout the Experiment [(µg·L^{-1})·d^{-1}]	SRP Decreasing Rate throughout the Experiment [(µg·L^{-1})·d^{-1}]
Control (no iron addition)	0.129 ± 0.017 (a)	*n.d.*	−0.80 ± 0.18 (a) $r^2 = 0.93$
T_{1P} (700 µ Fe·L^{-1})	0.444 ± 0.122 (b)	−28.64 ± 1.83 * $r^2 = 0.82$ −13.87 ± 4.72 ** (a) $r^2 = 0.92$	−1.29 ± 0.37 (a) $r^2 = 0.78$
T_{2P} (350 µ Fe·L^{-1} + 350 µ Fe·L^{-1})	0.580 ± 0.139 (b)	−17.60 ± 1.97 ** (a) $r^2 = 0.84$	−1.26 ± 0.58 (a) $r^2 = 0.72$

3.4. Total MC Concentration and MC Quota under Different Iron Addition Treatments

Data shown in this section only correspond to the samples collected during 2018 (second experiment) because of the negligible values of the MC concentrations in samples-2017 (first experiment; see Section 3.1). The total MC concentration and MC quota showed a distinctive response along the growth population curve. Moreover, different responses were observed according to treatments; *Microcystis* in the control showed a decreasing trend in the total MC concentration throughout the experiment (from 5.0 ± 0.01 to 1.38 ± 0.63 µg·L^{-1}; Figure 4A), coincident with a drop in the cell abundance (Figure 3A). On the other hand, *Microcystis* exposed to iron addition treatments (T_{1P} and T_{2P}) displayed an increment in the total MC concentration (from 5.18 ± 0.23 to 32.68 ± 14.65 or to 25.98 ± 10.05 µg·L^{-1} respectively; Figure 4A) along with a rise in cell abundance (Figure 3A). In particular, T_{1P} showed a significantly higher MC concentration (17.88 ± 2.15 µg·L^{-1}) than T_{2P} at day 15 (5.07 ± 0.59 µg·L^{-1}; $p \leq 0.05$; Figure 4A).

Regarding the MC quota, within the first week of the experiment (lag phase), no significant differences among iron treatments were observed, while cells under control conditions displayed significantly higher values at day 8 ($p \leq 0.05$; Figure 4B). However, we acknowledge that the high MC quota in the control set could be caused by a low cell division rate and MC accumulation, as we observed a significantly lower specific growth rate in comparison to that with iron treatments (Table 4). On the other hand, during the exponential phase, the MC quota decreased with all treatments at day 25 and was not significantly different among them. The latter is in accordance with [67] who observed a pronounced decline in intracellular MC after day 15 with all iron treatments. However, cells under different iron treatment conditions showed significant differences in the MC quota among each other over the exponential phase; cells treated with one iron addition pulse displayed values significantly higher at day 15 (T_{1P}; 0.40 ± 0.03 pg·$cell^{-1}$) in comparison with those in cells receiving a second iron pulse (T_{2P}; 0.13 ± 0.04 pg·$cell^{-1}$; $p \leq 0.05$; Figure 4B). Indeed, cells under T_{2P} conditions showed a significant decrease in the MC quota from day 8 to day 15, after the second iron pulse at day 9 ($p \leq 0.05$; Figure 4B). These results may indicate that different iron additions applied during the exponential phase

(T$_{1P}$: no pulse and T$_{2P}$: one pulse at day 9) could influence the MC content, reducing the production with an iron supply.
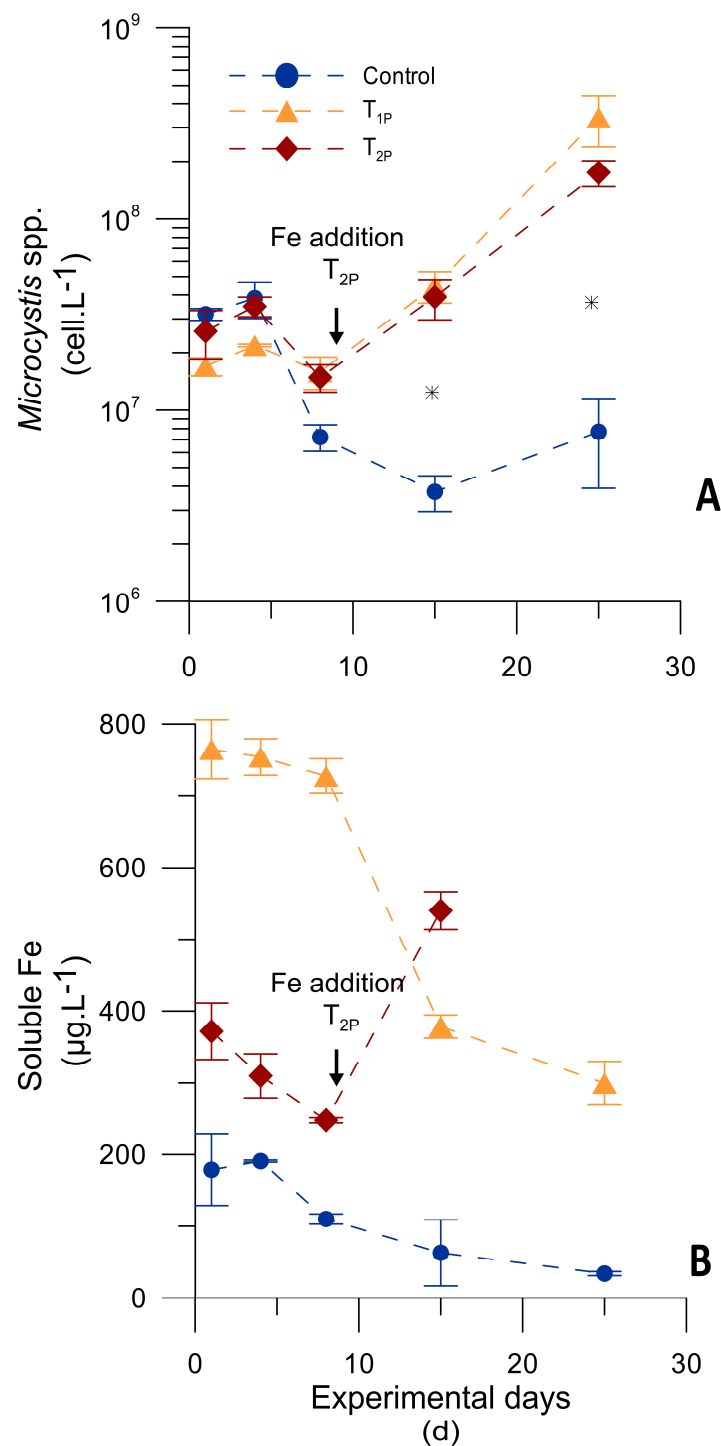

Figure 3. Cell abundance (cell·L^{-1}) (**A**) and soluble iron concentration (SFe; µg·L^{-1}) (**B**) in *Microcystis* spp. natural populations from sample-2018 under different treatments during the second experiment. Control, without iron addition (179 ± 25 µg Fe·L^{-1}); T$_{1P}$, with a single pulse: +700 µg Fe·L^{-1} at day 1 (D1); T$_{2P}$, the same amount divided in 2: +350 µg Fe·L^{-1} at D1 (first pulse) and 350 µg Fe·L^{-1} at day 9 (second pulse). Values are the means of triplicates, and vertical lines above symbols represent standard deviations. The SFe content in T$_{2P}$ is missing for day 25. Asterisks are located above the treatments that showed a significant difference in cell abundance in comparison with that in the other treatment groups (**A**).
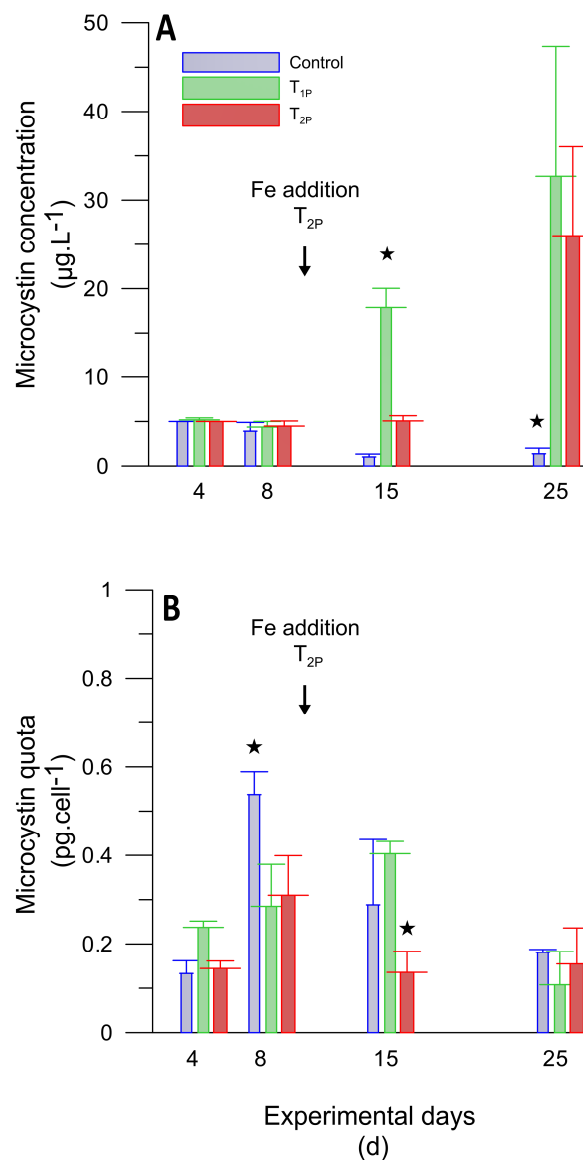
Figure 4. Microcystin (MC) concentration ($\mu g \cdot L^{-1}$) and MC quota ($pg \cdot cell^{-1}$) in *Microcystis* spp. natural populations from sample-2018 under the different treatment conditions during the second experiment. Control, without iron addition (179 ± 25 μg $Fe \cdot L^{-1}$); T_{1P}, with a single pulse: $+700$ μg $Fe \cdot L^{-1}$ at day 1 (D1); T_{2P}, the same amount divided in 2: $+350$ μg $Fe \cdot L^{-1}$ at D1 (first pulse) and 350 μg $Fe \cdot L^{-1}$ at day 9 (second pulse). Values are the means of triplicates, and vertical lines above bars are standard deviations. Asterisks are located above the treatments that showed a significant difference in the MC concentration (**A**) and MC quota (**B**) in comparison with those in the other treatment groups.

Regarding the growth of *Microcystis* spp. populations under low iron concentrations, MC synthesis has been proposed to give a selective advantage, as it may play a role in intracellular storage or as a transport peptide in iron metabolism [19,38]. In this way, toxic *Microcystis* strains might have a more efficient iron uptake system than the nontoxic *Microcystis* strains [36,37,59].

Although our results are in accordance with [36,38], who reported that the *M. aeruginosa* cells exposed to low iron levels displayed a higher intracellular concentration of MCs than cells under high iron conditions, we recognized that the differences in iron concentration between T_{1P} and T_{2P} were not so pronounced at day 15 (378 ± 16 and 540 ± 26 $\mu g \cdot Fe \cdot L^{-1}$

respectively). Hence, differences in the MC quota observed in our study could be not directly associated with the iron factor.

It is known that not all *Microcystis* strains are capable of toxin production and that during a bloom, a single species can shift the proportion of toxic and non-toxic cells [68]. Our results did not distinguish if the increase in the MC concentration under low levels of SFe was due to an increase in the proportion of toxic *Microcystis* in comparison with that of nontoxic *Microcystis* strains, instead of an increase in the MC quota. However, the cell abundance and MC concentration were positively correlated (R = 0.58, *p* < 0.001, n = 23), which would indicate that significant differences in MC concentrations among treatments might be caused mainly by the MC quota. In addition, many studies with *Microcystis* and *Planktothrix* natural populations showed that only 54% of the variation in MC concentrations could be explained by changes in the proportion of MC-producing cells, suggesting that a considerable part of the MC concentrations was also due to variations in the MC quota [69].

4. Conclusions

Our data showed that natural populations of *Microcystis* spp. under conditions of high temperature and sufficient light in the water column (e.g., austral summer and autumn season conditions), as well as under a high P supply (e.g., eutrophic reservoirs), appear to have growth responses driven by other factors, such as the iron supply. From our results of a *Microcystis* spp. natural population grown under optimal light, temperature, pH and P conditions and considering the range of iron concentrations in the subsurface layer of an eutrophic system, the San Roque reservoir, we conclude the following: 1. iron is a growth promoting factor; 2. the optimal range of iron concentrations for growth is between 700 and 1100 μg Fe·L^{-1}; 3. growth is not significantly different when iron is supplied in different modes (i.e.,:700 μg Fe·L^{-1} supplied in a single pulse at first day or in two pulses at the start and at the half of the experiment); 4. a clear relationship between the iron supply and MC quota is not demonstrated.

From our data, we recognized the iron supply (e.g., from internal sources) as an important factor determining the growth of populations of *Microcystis* spp. in eutrophic systems. Thus, it is essential to continue more studies related to the role of trace metals in cyanobacterial growth, bloom formation and the production of MCs in natural populations, in order to gain a better understanding of the potential effects of micronutrient internal sources on eutrophic systems.

References

1. Le Moal, M.; Gascuel-Odoux, C.; Ménesguen, A.; Souchon, Y.; Étrillard, C.; Levain, A.; Moatar, F.; Pannard, A.; Souchu, P.; Lefebvre, A.; et al. Eutrophication: A new wine in an old bottle? *Sci. Total Environ.* **2019**, *651*, 1–11. [CrossRef] [PubMed]
2. Smith, V.H.; Joye, S.B.; Howarth, R.W. Eutrophication of freshwater and marine ecosystems. *Limnol. Oceanogr.* **2006**, *51*, 351–355. [CrossRef]
3. Wurtsbaugh, W.A.; Paerl, H.W.; Dodds, W.K. Nutrients, eutrophication and harmful algal blooms along the freshwater to marine continuum. *WIREs Water* **2019**, *6*, e1373. [CrossRef]
4. Oliveira, M.; Machado, A.V. The role of phosphorus on eutrophication: A historical review and future perspectives. *Environ. Technol. Rev.* **2013**, *2*, 117–127. [CrossRef]
5. Rast, W.; Thornton, J.A. Trends in eutrophication research and control. *Hydrol. Process.* **1996**, *10*, 295–313. [CrossRef]
6. Schindler, D.W.; Hecky, R.E.; Findlay, D.L.; Stainton, M.P.; Parker, B.R.; Paterson, M.J.; Beaty, K.G.; Lyng, M.; Kasian, S.E.M. Eutrophication of lakes cannot be controlled by reducing nitrogen input: Results of a 37-year whole-ecosystem experiment. *Proc. Natl. Acad. Sci. USA* **2008**, *105*, 11254–11258. [CrossRef]
7. Dokulil, M.T.; Teubner, K. Cyanobacterial dominance in lakes. *Hydrobiologia* **2000**, *438*, 1–12. [CrossRef]
8. Moss, B.; Kosten, S.; Meerhoff, M.; Battarbee, R.W.; Jeppesen, E.; Mazzeo, N.; Havens, K.; Lacerot, G.; Liu, Z.; De Meester, L.; et al. Allied attack: Climate change and eutrophication. *Inland Waters* **2011**, *1*, 101–105. [CrossRef]
9. Paerl, H.W.; Paul, V.J. Climate change: Links to global expansion of harmful cyanobacteria. *Water Res.* **2012**, *46*, 1349–1363. [CrossRef]
10. Chen, L.; Giesy, J.P.; Adamovsky, O.; Svirčev, Z.; Meriluoto, J.; Codd, G.A.; Mijovic, B.; Shi, T.; Tuo, X.; Li, S.C.; et al. Challenges of using blooms of *Microcystis* spp. in animal feeds: A comprehensive review of nutritional, toxicological and microbial health evaluation. *Sci. Total Environ.* **2021**, *764*, 142319. [CrossRef]
11. Chorus, I.; Welker, M. (Eds.) *Toxic Cyanobacteria in Water: A Guide to Their Public Health Consequences, Monitoring and Management*, 2nd ed.; Taylor & Francis: London, UK, 2021.
12. Harke, M.J.; Steffen, M.M.; Gobler, C.J.; Otten, T.G.; Wilhelm, S.W.; Wood, S.A.; Paerl, H.W. A review of the global ecology, genomics, and biogeography of the toxic cyanobacterium, *Microcystis* spp. *Harmful Algae* **2016**, *54*, 4–20. [CrossRef]
13. Müller, M.N.; Mardones, J.I.; Dorantes-Aranda, J.J. Editorial: Harmful Algal Blooms (HABs) in Latin America. *Front. Mar. Sci.* **2020**, *7*, 34. [CrossRef]
14. Aguilera, A.; Haakonsson, S.; Martin, M.V.; Salerno, G.L.; Echenique, R.O. Bloom-forming cyanobacteria and cyanotoxins in Argentina: A growing health and environmental concern. *Limnologica* **2018**, *69*, 103–114. [CrossRef]
15. Ruibal-Conti, A.L.; Guerrero, J.M.; Regueira, J.M. Levels of microcystins in two Argentinean reservoirs used for water supply and recreation: Differences in the implementation of safe levels. *Environ. Toxicol. Int. J.* **2005**, *20*, 263–269. [CrossRef]
16. Ruiz, M.; Galanti, L.; Ruibal, A.L.; Rodriguez, M.I.; Wunderlin, D.A.; Amé, M.V. First report of microcystins and anatoxin-a co-occurrence in San Roque reservoir (Córdoba, Argentina). *Water Air Soil Pollut.* **2013**, *224*, 1593. [CrossRef]
17. Oberholster, P.J.; Botha, A.M.; Grobbelaar, J.U. *Microcystis aeruginosa*: Source of toxic microcystins in drinking water. *Afr. J. Biotechnol.* **2004**, *3*, 159–168. [CrossRef]
18. Pavlova, V.; Furnadzhieva, S.; Rose, J.; Andreeva, R.; Bratanova, Z.; Nayak, A. Effect of temperature and light intensity on the growth, chlorophyll a concentration and microcystin production by *Microcystis aeruginosa*. *Gen. Appl. Plant Physiol.* **2010**, *36*, 148–158.
19. Utkilen, H.; Gjølme, N. Iron-stimulated toxin production in *Microcystis aeruginosa*. *Appl. Environ. Microbiol.* **1995**, *61*, 797–800. [CrossRef]
20. Benayache, N.-Y.; Nguyen-Quang, T.; Hushchyna, K.; McLellan, K.; Afri-Mehennaoui, F.-Z.; Bouaïcha, N. An overview of cyanobacteria harmful algal bloom (CyanoHBA) issues in freshwater ecosystems. In *Limnology- Some New Aspects of Inland Water Ecology*; IntechOpen: London, UK, 2019; pp. 13–37.
21. Davis, T.W.; Berry, D.L.; Boyer, G.L.; Gobler, C.J. The effects of temperature and nutrients on the growth and dynamics of toxic and non-toxic strains of *Microcystis* during cyanobacteria blooms. *Harmful Algae* **2009**, *8*, 715–725. [CrossRef]
22. Downing, J.A.; Watson, S.B.; McCauley, E. Predicting cyanobacteria dominance in lakes. *Can. J. Fish. Aquat. Sci.* **2001**, *58*, 1905–1908. [CrossRef]
23. Gobler, C.J.; Burkholder, J.M.; Davis, T.W.; Harke, M.J.; Johengen, T.; Stow, C.A.; Van de Waal, D.B. The dual role of nitrogen supply in controlling the growth and toxicity of cyanobacterial blooms. *Harmful Algae* **2016**, *54*, 87–97. [CrossRef] [PubMed]
24. Harris, T.D.; Wilhelm, F.M.; Graham, J.L.; Loftin, K.A. Experimental manipulation of TN: TP ratios suppress cyanobacterial biovolume and microcystin concentration in large-scale in situ mesocosms. *Lake Reserv. Manag.* **2014**, *30*, 72–83. [CrossRef]
25. Amé, M.V.; Wunderlin, D.A. Effects of iron, ammonium and temperature on microcystin content by a natural concentrated *Microcystis aeruginosa* population. *Water Air Soil Pollut.* **2005**, *168*, 235–248. [CrossRef]

26. Dai, R.; Wang, P.; Jia, P.; Zhang, Y.; Chu, X.; Wang, Y. A review on factors affecting microcystins production by algae in aquatic environments. *World J. Microbiol. Biotechnol.* **2016**, *32*, 51. [CrossRef]

27. Facey, J.A.; Apte, S.C.; Mitrovic, S.M. A review of the effect of trace metals on freshwater cyanobacterial growth and toxin production. *Toxins* **2019**, *11*, 643. [CrossRef]

28. Lukač, M.; Aegerter, R. Influence of trace metals on growth and toxin production of *Microcystis aeruginosa*. *Toxicon* **1993**, *31*, 293–305. [CrossRef]

29. Jiang, Y.; Ji, B.; Wong, R.N.S.; Wong, M.H. Statistical study on the effects of environmental factors on the growth and microcystin production of bloom-forming cyanobacterium-*Microcystis aeruginosa*. *Harmful Algae* **2008**, *7*, 127–136. [CrossRef]

30. Steffen, M.M.; Belisle, B.S.; Watson, S.B.; Boyer, G.L.; Wilhelm, S.W. Status, causes and controls of cyanobacterial blooms in Lake Erie. *J. Great Lakes Res.* **2014**, *40*, 215–225. [CrossRef]

31. Berman-Frank, I.; Quigg, A.; Finkel, Z.V.; Irwin, A.J.; Haramaty, L. Nitrogen-fixation strategies and Fe requirements in cyanobacteria. *Limnol. Oceanogr.* **2007**, *52*, 2260–2269. [CrossRef]

32. Glass, J.B.; Wolfe-Simon, F.; Anbar, A.D. Coevolution of metal availability and nitrogen assimilation in cyanobacteria and algae. *Geobiology* **2009**, *7*, 100–123. [CrossRef]

33. Molot, L.A.; Watson, S.B.; Creed, I.F.; Trick, C.G.; Mccabe, S.K.; Verschoor, M.J.; Sorichetti, R.J.; Powe, C.; Venkiteswaran, J.J.; Schiff, S.L. A novel model for cyanobacteria bloom formation: The critical role of anoxia and ferrous iron. *Freshw. Biol.* **2014**, *59*, 1323–1340. [CrossRef]

34. Ceballos-Laita, L.; Marcuello, C.; Lostao, A.; Calvo-Begueria, L.; Velazquez-Campoy, A.; Bes, M.T.; Fillat, M.F.; Peleato, M.L. Microcystin-LR binds iron, and iron promotes self-assembly. *Environ. Sci. Technol.* **2017**, *51*, 4841–4850. [CrossRef]

35. Martin-Luna, B.; Sevilla, E.; Hernandez, J.A.; Bes, M.T.; Fillat, M.F.; Peleato, M.L. Fur from *Microcystis aeruginosa* binds in vitro promoter regions of the microcystin biosynthesis gene cluster. *Phytochemistry* **2006**, *67*, 876–881. [CrossRef]

36. Alexova, R.; Fujii, M.; Birch, D.; Cheng, J.; Waite, T.D.; Ferrari, B.C.; Neilan, B.A. Iron uptake and toxin synthesis in the bloom-forming *Microcystis aeruginosa* under iron limitation. *Environ. Microbiol.* **2011**, *13*, 1064–1077. [CrossRef]

37. Lyck, S.; Gjølme, N.; Utkilen, H. Iron starvation increases toxicity of *Microcystis aeruginosa* CYA 228/1 (Chroococcales, Cyanophyceae). *Phycologia* **1996**, *35*, 120–124. [CrossRef]

38. Sevilla, E.; Martin-Luna, B.; Vela, L.; Bes, M.T.; Fillat, M.F.; Peleato, M.L. Iron availability affects mcyD expression and microcystin-LR synthesis in *Microcystis aeruginosa* PCC7806. *Environ. Microbiol.* **2008**, *10*, 2476–2483. [CrossRef]

39. Buratti, F.M.; Manganelli, M.; Vichi, S.; Stefanelli, M.; Scardala, S.; Testai, E.; Funari, E. Cyanotoxins: Producing organisms, occurrence, toxicity, mechanism of action and human health toxicological risk evaluation. *Arch. Toxicol.* **2017**, *91*, 1049–1130. [CrossRef]

40. Geng, L.; Qin, B.; Yang, Z. Unicellular *Microcystis aeruginosa* cannot revert back to colonial form after short-term exposure to natural conditions. *Biochem. Syst. Ecol.* **2013**, *51*, 104–108. [CrossRef]

41. Wu, Z.X.; Song, L.R. Physiological comparison between colonial and unicellular forms of *Microcystis aeruginosa* Kütz.(Cyanobacteria). *Phycologia* **2008**, *47*, 98–104. [CrossRef]

42. Xiao, M.; Li, M.; Reynolds, C.S. Colony formation in the cyanobacterium Microcystis. *Biol. Rev.* **2018**, *93*, 1399–1420. [CrossRef]

43. Quirós, R.; Drago, E. The environmental state of Argentinean lakes: An overview. *Lakes Reserv. Res. Manag.* **1999**, *4*, 55–64. [CrossRef]

44. Rodríguez, M.I.; Ruiz, M. Limnology of the San Roque Reservoir. In *The Suquía River Basin (Córdoba, Argentina). The Handbook of Environmental Chemistry*; Wunderlin, D., Ed.; Springer: Cham, Switzerland, 2016; pp. 37–59. [CrossRef]

45. Halac, S.; Mengo, L.; Guerra, L.; Lami, A.; Musazzi, S.; Loizeau, J.L.; Ariztegui, D.; Piovano, E.L. Paleolimnological reconstruction of the centennial eutrophication processes in a sub-tropical South American reservoir. *J. South Am. Earth Sci.* **2020**, *103*, 102707. [CrossRef]

46. Cao, Z.; Li, P.; Li, Z.H. A latest review on the application of microcosm model in environmental research. *Environ. Sci. Pollut. Res.* **2021**, *28*, 60438–60447. [CrossRef] [PubMed]

47. Belzile, N.; Chen, Y.; Gunn, J.M.; Tong, J.; Alarie, Y.; Delonchamp, T.; Lang, C. The effect of selenium on mercury assimilation by freshwater organisms. *Can. J. Fish. Aquat. Sci.* **2006**, *63*, 1–10. [CrossRef]

48. INA-SCIRSA. Characterization of Water Quality and Meteorological Variables Related to Cyanobacterial Extreme Bloom Events in the San Roque Reservoir. 2018. Available online: https://www.ina.gov.ar/archivos/publicaciones/2018_Pussetto%20et%20al_Caracterizaci%C3%B3n%20Calidad%20Agua%20Eventos%20Extremos.pdf (accessed on 28 October 2022).

49. Amaral, V.; Bonilla, S.; Aubriot, L. Growth optimization of the invasive cyanobacterium *Cylindrospermopsis raciborskii* in response to phosphate fluctuations. *Eur. J. Phycol.* **2014**, *49*, 134–141. [CrossRef]

50. Vogel, A.; Jeffery, G.H. Fundamental theoretical principles of reactions in solutions. In *Vogel's Textbook of Quantitative Chemical Analysis*; Wiley and Sons: New York, NY, USA, 1989; pp. 15–70.

51. APHA. *Standard Methods: For the Examination of Water and Waste Water*, 23rd ed.; American Public Health Association: Washington, DC, USA, 2017. [CrossRef]

52. Hillebrand, H.; Dürselen, C.-D.; Kirschtel, D.; Pollingher, U.; Zohary, T. Biovolume calculation for pelagic and benthic microalgae. *J. Phycol.* **1999**, *35*, 403–424. [CrossRef]

53. Zar, J.H. Statistical significance of mutation frequencies, and the power of statistical testing, using the poisson distribution. *Biom. J.* **1984**, *26*, 83–88. [CrossRef]

54. R Core Team. *R: A Language and Environment for Statistical Computing*; R Foundation for Statistical Computing: Vienna, Austria, 2020. Available online: https://www.R-project.org/ (accessed on 28 October 2022).

55. Puddick, J.; Thomson-Laing, G.; Wood, S.A. Microcystins in New Zealand: A review of occurrence, congener diversity and cell quotas. *New Zealand. J. Bot.* **2019**, *57*, 93–111. [CrossRef]

56. Almanza, V.; Pedreros, P.; Laughinghouse, H.D.; Félez, J.; Parra, O.; Azócar, M.; Urrutia, R. Association between trophic state, watershed use, and blooms of cyanobacteria in south-central Chile. *Limnologica* **2019**, *75*, 30–41. [CrossRef]

57. Halac, S.; Bazán, R.; Larrosa, N.; Nadal, A.F.; Ruibal Conti, A.L.; Rodríguez, M.I.; Ruiz, M.; Lopéz, A.G. First report on negative association between cyanobacteria and fecal indicator bacteria at San Roque reservoir (Argentina): Impact of environmental factors. *J. Freshw. Ecol.* **2019**, *34*, 273–291. [CrossRef]

58. Whitton, B.A.; Potts, M. Introduction to the Cyanobacteria. In *The Ecology of Cyanobacteria: Their Diversity in Time and Space*; Whitton, B.A., Potts, M., Eds.; Springer: Berlin/Heidelberg, Germany, 2007. [CrossRef]

59. Fujii, M.; Rose, A.L.; David Waite, T. Iron uptake by toxic and nontoxic strains of *Microcystis aeruginosa*. *Appl. Environ. Microbiol.* **2011**, *77*, 7068–7071. [CrossRef]

60. Xing, W.; Huang, W.; Li, D.; Liu, Y. Effects of iron on growth, pigment content, photosystem II efficiency, and siderophores production of Microcystis aeruginosa and *Microcystis wesenbergii*. *Curr. Microbiol.* **2007**, *55*, 94–98. [CrossRef]

61. Walsby, A.E.; McAllister, G.K. Buoyancy regulation by *Microcystis* in Lake Okaro. *N. Z. J. Mar. Freshw. Res.* **1987**, *21*, 521–524. [CrossRef]

62. Ibelings, B.W.; Mur, L.R.; Walsby, A.E. Diurnal changes in buoyancy and vertical distribution in populations of *Microcystis* in two shallow lakes. *J. Plankton Res.* **1991**, *13*, 419–436. [CrossRef]

63. Paerl, H.W.; Otten, T.G. Harmful Cyanobacterial Blooms: Causes, Consequences, and Controls. *Microb. Ecol.* **2013**, *65*, 995–1010. [CrossRef]

64. Tammeorg, O.; Nürnberg, G.; Niemistö, J.; Haldna, M.; Horppila, J. Internal phosphorus loading due to sediment anoxia in shallow areas: Implications for lake aeration treatments. *Aquat. Sci.* **2020**, *82*, 1–10. [CrossRef]

65. Visser, P.M.; Ibelings, B.W.; Mur, L.R.; Walsby, A.E. The ecophysiology of the harmful cyanobacterium *Microcystis*. In *Harmful Cyanobacteria*; Huisman, J., Matthijs, H.C.P., Visser, P.M., Eds.; Springer: Dordrecht, The Netherlands, 2005; pp. 109–142. [CrossRef]

66. Bormans, M.; Sherman, S.; Webster, I.T. Is buoyancy regulation in cyanobacteria an adaptation to exploit separation of light and nutrients? *Mar. Freshw. Res.* **1999**, *50*, 897–906. [CrossRef]

67. Li, H.; Murphy, T.; Guo, J.; Parr, T.; Nalewajko, C. Iron-stimulated growth and microcystin production of *Microcystis novacekii* UAM 250. *Limnologica* **2009**, *39*, 255–259. [CrossRef]

68. Wood, S.A.; Dietrich, D.R.; Craig Cary, S.; Hamilton, D.P. Increasing *Microcystis* cell density enhances microcystin synthesis: A mesocosm studies. *Inland Waters* **2012**, *2*, 17–22. [CrossRef]

69. Sabart, M.; Pobel, D.; Briand, E.; Combourieu, B.; Salençon, M.J.; Humbert, J.F.; Latour, D. Spatiotemporal variations in microcystin concentrations and in the proportions of microcystin-producing cells in several *Microcystis aeruginosa* populations. *Appl. Environ. Microbiol.* **2010**, *76*, 4750–4759. [CrossRef]